

AD-A271 324

12

DEFENSE TECHNICAL INFORMATION CENTER



A271324

ABSOLUTE POSITIONING BY COLLECTING GLOBAL POSITIONING SYSTEM (GPS) DATA ALONG SHORT BASELINES

BY BRUCE R. HERMANN AND ALAN G. EVANS
STRATEGIC AND SPACE SYSTEMS DEPARTMENT

SEPTEMBER 1993

DTIC
ELECTE
OCT 22 1993
S A D

Approved for public release; distribution is unlimited.



NAVAL SURFACE WARFARE CENTER
DAHLGREN DIVISION
Dahlgren, Virginia 22448-5000

93-25514



93 10 21 089

NSWCDD/TR-93/309

**ABSOLUTE POSITIONING BY COLLECTING
GLOBAL POSITIONING SYSTEM (GPS) DATA
ALONG SHORT BASELINES**

**BY BRUCE R. HERMANN AND ALAN G. EVANS
STRATEGIC AND SPACE SYSTEMS DEPARTMENT**

SEPTEMBER 1993

Approved for public release; distribution is unlimited.

**NAVAL SURFACE WARFARE CENTER
DAHLGREN DIVISION
Dahlgren, Virginia 22448-5000**

FOREWORD

One mission of the Defense Mapping Agency (DMA) requires the determination of near real time geodetic quality absolute positions in areas far removed from data processing stations. It has been demonstrated that a few hours of observations from the Global Positioning System (GPS) constellation can provide static point position solutions accurate to within 3 to 4 m when processing is performed with an uncorrupted broadcast ephemeris and two frequency data. When the GPS is operating with AntiSpoofing (AS) and Selective Availability (SA), these high-quality solutions are not possible unless the equipment can accommodate cryptokeys and the necessary positioning algorithms reside within the receiver. Since it is more convenient to operate without the overhead of cryptokeys and in an unclassified environment, this report investigates whether high-quality absolute positions are possible using unconventional techniques with unclassified equipment in the presence of AS and SA.

Support was provided by DMA under the direction of Mr. B. Roth and Mr. S. Malys.

This report has been reviewed by Dr. J. Blanton, Head, Space and Geodesy Branch; Mr. T. Sims, Head, Space Sciences Branch; and Mr. J. Sloop, Head, Space and Surface Systems Division.

Accession For	
NTIS	CRA&I <input checked="" type="checkbox"/>
DTIC	TabE <input type="checkbox"/>
Unannounced <input type="checkbox"/>	
JST Distribution	
By _____	
Distribution/	
Availability Group	
Dist	Availability Group
A-1	

Approved by:

R. L. Schmidt

R. L. SCHMIDT, Head
Strategic and Space Systems Department

DTIC QUALITY INSPECTED 2

ABSTRACT

This report addresses the problem of determining absolute positions (longitude and latitude) from Global Positioning System (GPS) data in the presence of Selective Availability (SA). The SA-epsilon effect can be avoided if one can wait until corrected or post-fitted satellite ephemerides and clock estimates become available. However, the SA-dither effect cannot easily be eliminated from the ranging data in the field. This report considers both problems and suggests methods that have the potential to allow absolute position solutions to be obtained even with dither corrupting the satellite data. The requirements and practicality of each are reviewed.

CONTENTS

	<u>Page</u>
MOTIVATION	1
BENEFIT EXPECTED FROM SUCH A TECHNIQUE	1
TECHNIQUES REVIEWED	2
PRELIMINARY ANALYSIS	4
POLE NORMAL TO THE GEOID	5
POINTING AND RANGING TO A KNOWN LANDMARK	9
POINTING TO A STELLAR OBJECT	10
INTERFEROMETRIC GPS OBSERVATIONS	10
MINIMIZING THE RESIDUAL OF FIT	13
MULTIPLE BASELINE EXPERIMENT	15
GPS AND LEVELING	25
SUMMARY	30
REFERENCES	31
DISTRIBUTION	(1)

MOTIVATION

Geodetic surveying of fixed points with the Global Positioning System (GPS) uses the satellite constellation to relate the coordinates of a point being surveyed to the World Geodetic System (WGS84) coordinate system. The first half of the link between the point and the coordinate system depends upon the observations of pseudoranges and/or phase to locate the point with respect to the constellation of satellites. The second half of the link locates the satellites in space and time with respect to the monitor stations whose positions are precisely known in the WGS84 coordinate system. With the Department of Defense Selective Availability (SA) in operation, both of these links are purposely corrupted. The SA-dither introduces errors that appear as random range errors on the observations and weakens the link between the site to be surveyed and the satellites. The SA-epsilon introduces errors into the satellite ephemerides and weakens the link between the satellites and the coordinate system.

Because the removal of the SA effects in the field requires additional cost and operational difficulty, it is assumed that the user would prefer to operate without that overhead. GPS receivers that do not have the capability to remove the SA effects are less expensive to purchase and can be operated on the L_1 frequency in an unclassified mode. Under normal operations with these receivers, the SA-epsilon effect can be avoided if one can wait to do the data processing until post-fitted satellite ephemerides become available from a third party. However, the SA-dither effect cannot be removed from the ranging data except in a secure environment. This report addresses the dither problem and investigates methods that may allow absolute position solutions to be obtained even with dither corrupting the satellite data.

The AntiSpoofing (AS) encryption will not be addressed. AS prevents access to the precise code (P-code) on both L_1 and L_2 frequencies. The Coarse Acquisition (C/A) code is available at all times, but only on the L_1 frequency, and is subject to the SA degradation described above.

BENEFIT EXPECTED FROM SUCH A TECHNIQUE

When SA is on and AS is either on or off, unclassified civilian receivers can still be used to collect GPS ranging data to do absolute positioning if

1. Single frequency C/A code is used.
2. SA-epsilon is avoided by using a post fit precise ephemerides.

3. The measurement system is designed to be insensitive to SA-dither.

The quality of the absolute position solutions so obtained was examined based upon an experiment performed at the Naval Surface Warfare Center, Dahlgren Division (NSWCDD). It cannot be expected and it has not been demonstrated that solutions can be obtained that are comparable to the level of accuracy attainable when SA is not in use.

TECHNIQUES REVIEWED

It has been demonstrated that collecting GPS data with two or more antennas in the relative positioning mode results in solutions for short baselines that are accurate and repeatable to within about 1 mm. The differencing of the phase observations between the antennas makes this method insensitive to errors due to satellite position, propagation effects, satellite clock variations, and SA-dither. Whereas the insensitivity is a benefit for precise relative positioning, the method makes it difficult to say anything about the absolute location of the baseline. Relative positioning gives a baseline vector that is precise in length and direction, but is free to translate through large distances in space.

Processing large quantities of GPS observations obtained over short baselines may help resolve the location of the observer if the dominant source of error is random. However, this method is inherently weak. What is helpful for absolute positioning is some additional observation that is correlated, in an absolute sense, with a point on the earth. This auxiliary observation, along with the vector baseline, would be used to pinpoint the location from which the observations were made. The acceptable accuracy for this new scheme must be better than that available from GPS single-frequency Standard Positioning Service (SPS) when SA is active. It should be able to routinely achieve 20 m Root Summed Square (RSS) with a goal of 5 m.

Geodetic quality absolute positioning requires precise pseudorange or range difference data and precise satellite ephemerides and clock estimates. The absolute position of the unknown point is found by collecting data from several satellites over a period of time. This provides the link from the user to the satellites. The satellite positions are known from the satellite ephemerides that are uploaded by the GPS Control Segment and transmitted to the user in real time. A globally distributed array of monitor sites, whose positions are known, receive data from the satellites on a continuous basis. These data allow the past satellite positions to be estimated and the future positions to be predicted. These ephemerides provide the link between the earth and the satellites. In effect, the user is positioning an unknown site with respect to the global array of monitor sites with the GPS satellites acting as an intermediary.

When relative positioning techniques are used, the absolute link to the monitor sites is weak and an alternate link to the earth is required. Several auxiliary observations that have been considered include the following:

1. Physically position the baseline so that it is normal to the geoid. The normal to the geoid could be transformed to the equivalent normal to the ellipsoid through the application of local deflections of the vertical. If this could be accomplished precisely, the observed vector baseline would take on a direction that is unique to some particular point on earth. The geodetic longitude and latitude could then be computed through the equation for the ellipsoid normal.
2. Pointing the GPS baseline at some object whose absolute position is known also gives a means for finding the location of the observer, if the range can also be determined. The range can be found by electronic distance measurement devices. This scheme can be very useful in a local area where some previously surveyed landmark is prominent.
3. Employing astronomical objects as angle references could be another scheme. The GPS antennas mounted on a telescope or other pointing device could be aimed directly at some astronomical object whose coordinates are known. Observations of several baseline vectors directed at different objects should be enough to uniquely determine the observer's location.
4. Precise optical astronomical observations are always dependent upon weather conditions; therefore, a similar technique utilizing all-weather radio observations would be more desirable. Radio interferometry may be used to replace the optical measurements described above with the positions of the GPS satellites.
5. Collect data from one or more baselines separated by moderate distances and perform conventional double difference processing to determine the baseline vectors, hold the vectors fixed, and reprocess the data with the absolute position of a reference antenna as the unknown. No auxiliary measurements are necessary for this technique.
6. GPS and leveling data are collected along two baselines radiating outward from a fixed site and preferably separated by about 90 deg. Tangents to the WGS84 ellipsoid model are formed by subtracting the leveling difference in height along the baseline from the GPS-determined height and correcting for both the Earth's curvature and deflections of the vertical. The latitude and longitude of the fixed point is found from the ellipsoid normal vector. The normal is computed from the cross product of the two tangent vectors obtained from the baseline vectors.

A brief description of each technique will be presented following the preliminary analysis.

PRELIMINARY ANALYSIS

The formulation presented below outlines the procedure for processing the data received by the GPS receiver(s) from the two antennas. The observation equation is written in the form suggested by Braasch:¹

$$P_r = P_s + c (T_{rcvr} - T_{sv}) + d_{tropo} + d_{iono} + d_{rel} + URE + d_{mp} + d_{HW} + d_{meas} + noise + SA \quad (1)$$

where the symbols represent the following:

- P_r = observed pseudorange as observed by the receiver (m)
- P_s = true geometric range between satellite and antenna (m)
- T_{rcvr} = receiver clock offset from GPS time (sec)
- T_{sv} = satellite clock offset from GPS time (sec)
- d_{tropo} = propagation delay caused by the troposphere (m)
- d_{iono} = propagation delay caused by the ionosphere (m)
- d_{rel} = satellite relativity correction (m)
- URE = User Range Error (satellite ephemeris and clock errors projected onto the range direction) (m)
- d_{mp} = multipath error (m)
- d_{HW} = receiver hardware delay (m)
- d_{meas} = receiver measurement bias errors (m)
- $noise$ = receiver measurement noise (m)
- SA = Selective Availability epsilon and dither (m)

For the purposes of the report, the following terms will be ignored: d_{tropo} , d_{rel} , URE , d_{HW} , and $noise$. The SA term will be expanded into its component parts: $SA_\epsilon = SA\text{-epsilon}$ and $SA_\delta = SA\text{-dither}$. The remaining terms will be retained but subscripts will be added to indicate time i , satellite j , and antenna k .

$$P_{ijk}(t_i) = P_{sjk}(t_i) + c [T_{rcvrk}(t_i) - T_{svj}(t_i)] + d_{ionojk}(t_i) + d_{measjk} + d_{mpjk} + SA_{\epsilon j}(t_i) + SA_{\delta j}(t_i) \quad (2)$$

In Equation (2), the term $P_{sjk}(t_i)$ is the magnitude of the difference between the vector to satellite j , represented by $r_{sj}(t_i)$, and the vector to the antenna receiving the signal $r_{ak}(t_i)$.

$$P_{sjk} = | r_{sj}(t_i) - r_{ak}(t_i) | \quad (3)$$

Next, collect data from the same satellites with the two antennas. Difference the data between the two antennas to remove the satellite dependent variables, including both components of SA. The differenced observation equation is

$$\Delta P_{rj}(t_i) = P_{sj1}(t_i) - P_{sj2}(t_i) + c [T_{rcvr1}(t_i) - T_{rcvr2}(t_i)] + d_{measj1} - d_{measj2} + d_{iono j1} - d_{iono j2} + d_{mpj1} - d_{mpj2} \quad (4)$$

Continuing with the second difference between satellites m and n results in Equation (5). Now there is no contribution from the local clock.

$$\Delta P_r(t_i) = P_{sm1}(t_i) - P_{sm2}(t_i) - [P_{sn1}(t_i) - P_{sn2}(t_i)] + d_{meas m1} - d_{meas m2} - [d_{meas n1} - d_{meas n2}] + d_{iono m1} - d_{iono m2} - [d_{iono n1} - d_{iono n2}] + d_{mp m1} - d_{mp m2} - [d_{mp n1} - d_{mp n2}] \quad (5)$$

When two receivers are used and synchronized by the same frequency standard, double differencing to remove receiver-dependent terms may not be necessary. In this case, there is just one local time offset variable instead of two (T_{rcvr1} and T_{rcvr2}) and that term in Equation (4) disappears. What is left is integer count offsets for each of the satellites and differences between the measurements noises, refraction effects, and multipath. The ranges P_{sj1} and P_{sj2} are functions of the x, y, z components of the satellite positions and the coordinates of the antennas.

POLE NORMAL TO THE GEOID

One solution to the problem of minimizing the effects of SA-dither on absolute position solutions requires that a short baseline, whose end points are defined by the phase centers of two GPS antennas, be oriented so that it is normal to the geoid. Since the phase centers of the antennas are not precisely known with respect to their physical structure, there will be an unavoidable uncertainty in identifying when the baseline is in fact normal to the geoid. It must be normal with a high degree of accuracy because it defines a unique vector at that particular location. This vector is unique because there is only one vector normal to the geoid at any given point. A diagram of the situation is shown in Figure 1. Three surfaces are illustrated: the equipotential surface called the *geoid*, the mathematical surface called the *ellipsoid*, and the physical surface labeled the *terrain*. The two vectors at the point P_0 represent the ellipsoid normal and the geoid normal. The angular difference between the two normals is called the deflection of the vertical ϵ . It can be seen that ϵ changes from point to point due the continuously changing directions between the two normal vectors.

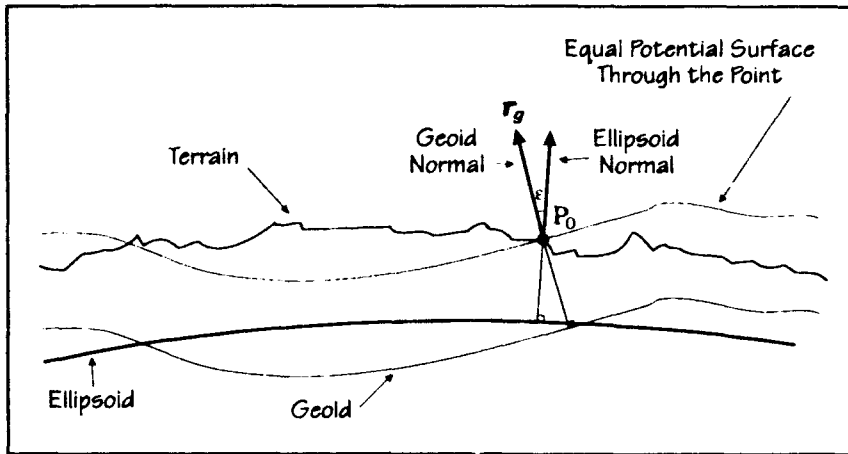


FIGURE 1. NORMALS TO THE ELLIPSOID AND THE GEOID AT A POINT P_0

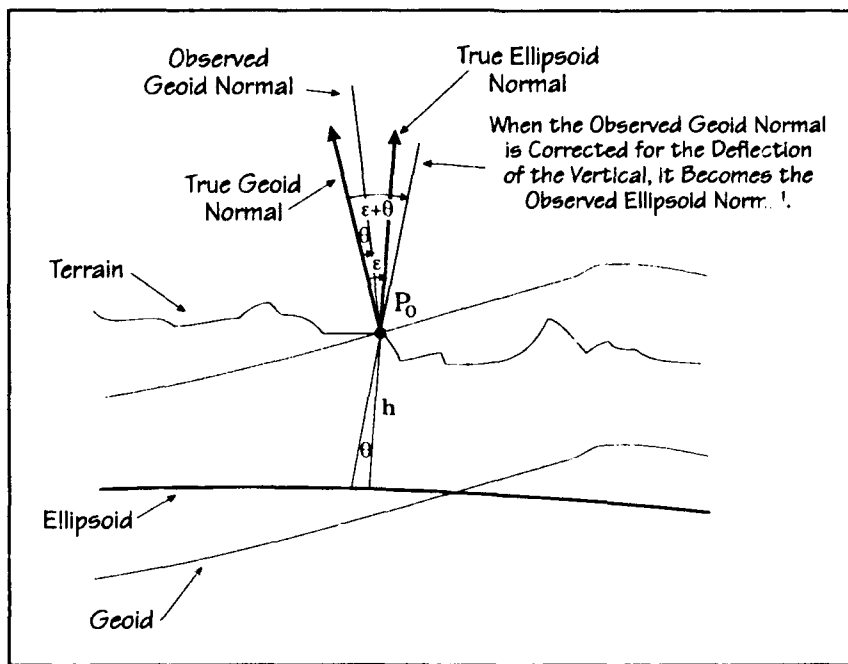


FIGURE 2. ERROR θ IN THE DETERMINATION OF THE GEOID NORMAL

In order to determine the geodetic absolute position, the normal to the ellipsoid at P_0 must be known. Assuming that the baseline formed by the GPS antennas can be made to coincide with the local normal to the geoid, GPS will provide the geodetic components for that vector: x_g , y_g , and z_g as in Equation (6). Additional information about the deflection of the vertical is then required to transform the true geoid normal into a true ellipsoid normal as shown by the application of the angle ϵ in Figure 2. From the approximate absolute position solution obtained using the conventional GPS SPS, the vertical deflection angles ξ and η (where accurately known) can be found from a table. The angles ξ and η are the east and north components of ϵ . After this operation, the ellipsoid normal unit vector \hat{u} can be used with Equation (7) to solve for the geodetic longitude λ and latitude ϕ .

$$\mathbf{r}_g = x_g \hat{x} + y_g \hat{y} + z_g \hat{z} \quad (6)$$

$$\hat{u} = \cos\phi \cos\lambda \hat{x} + \cos\phi \sin\lambda \hat{y} + \sin\phi \hat{z} \quad (7)$$

If the geoid normal is not fully determined and as a result there is an error θ in its direction as illustrated in Figure 2, application of the corrections for the deflections of the vertical will propagate the error into the observed ellipsoid normal; then the result is an error θ in the ellipsoid normal vector. Under these conditions, when Equation (2) is used to determine the longitude and latitude of the point P_0 , the error may be considerable because the position for which the observed ellipsoid normal is the true normal may be quite distant. This is illustrated on an ellipsoid with an exaggerated eccentricity in Figure 3. The place where the observed ellipsoid normal is actually normal to the ellipsoid is the point P_1 . In addition, the residual errors in the deflection of the vertical at P_0 will degrade the accuracy of this process.

In order to put the problem on a firmer foundation, a numerical example follows. Suppose that the error in the determination of the baseline vector is 1 mm in the direction perpendicular to the true normal. Assuming a baseline length of 1 m, the angular error incurred is 1 mrad (angle θ in Figure 2). If the deflection of the vertical is perfectly compensated, then the error in the ellipsoid normal is also 1 mrad. For numerical simplicity, the point P_0 will be placed at longitude, latitude, and ellipsoidal height equal to zero. This is on the equator at the intersection of the plane formed by the x and z axes of the WGS84 coordinate system. In this case, the true unit vector from Equation (7) is $\hat{u}_t = \hat{x}$. The observed unit vector, which includes the 1-mrad error, is \hat{u}_o with components $x_{uo}=0.9999995$, $y_{uo}=0.001$, and $z_{uo}=0$.

$$\hat{u}_o = x_{uo} \hat{x} + y_{uo} \hat{y} + z_{uo} \hat{z} \quad (8)$$

Solving by equating components in Equations (7) and (8), gives the latitude as zero because there is no \hat{z} component. Solving for longitude from either of the other two components gives an observed longitude of 0.05729578 deg. This is equivalent to a 1-mrad longitude error.

which is the same magnitude as the error in the ellipsoid normal. A similar result in latitude is obtained if all the error is put in z_{uo} . No matter how the error is distributed, the angular position error on the ellipsoid is equivalent to the magnitude of the angular error in the baseline vector. In this example, if the magnitude of the vector from the origin to the point P_0 is given by Equation (9), then r_0 is 6378135 m, and the position error on the surface of the ellipsoid is approximately 6378.135 m.

$$r_0 = \sqrt{x_{P_0}^2 + y_{P_0}^2 + z_{P_0}^2} \quad (9)$$

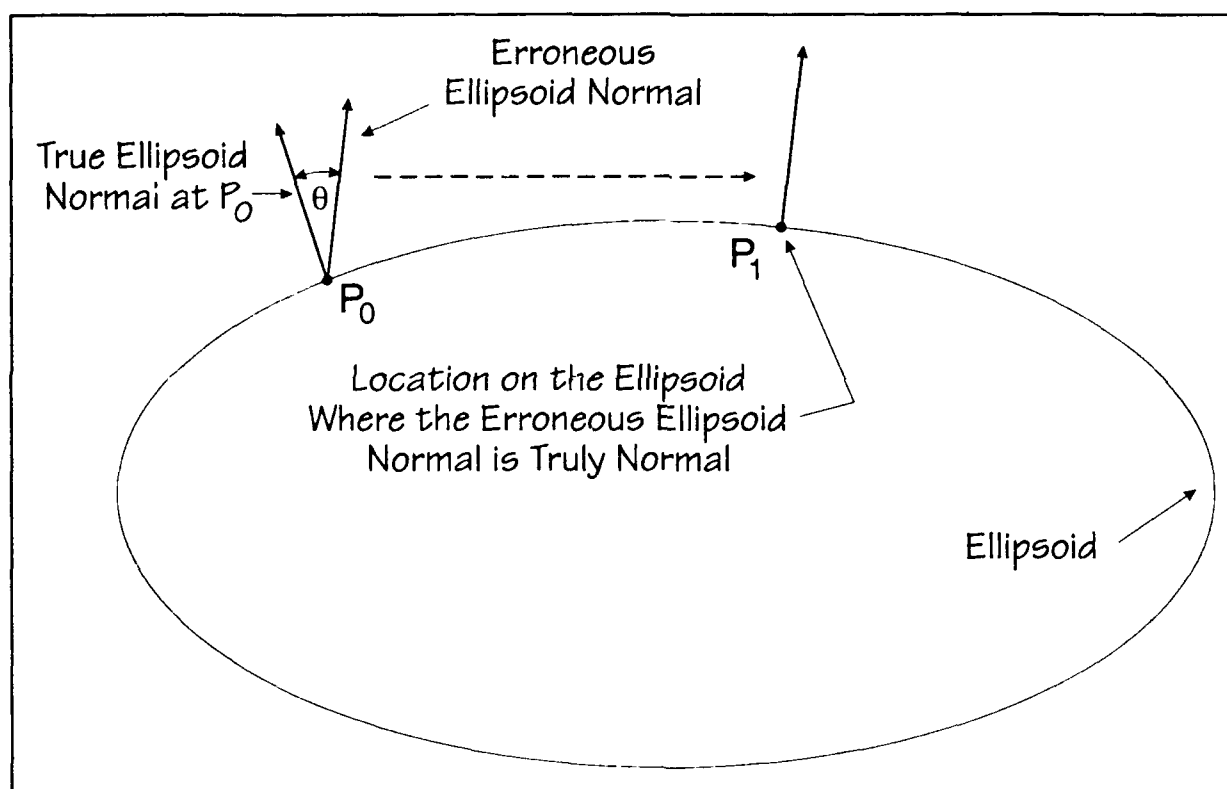


FIGURE 3. POSITION ERROR DUE TO AN ERROR θ IN THE OBSERVED ELLIPSOID NORMAL

This technique is very sensitive to errors incurred when the GPS antennas are set up to form a baseline perpendicular to the geoid. A small error in this placement translates directly into a position error equal to that angular error multiplied by r_0 . The fact that the ellipsoid normal and the *observed* ellipsoid normal differ by a distance approximately equal to the angular error θ multiplied by the height of the terrain above the ellipsoid (h) is not relevant when Equation (2) is being used to determine the geodetic position. Even in the case where the terrain and the geoid

coincide with the ellipsoid ($h=0$), an angular error θ in the observed normal vector would still cause an error in the determination of the geodetic position.

In this application, with GPS baselines on the order of 1 m, the errors in the vector direction will be on the order of 1 mrad. Given that the other errors will be added to this, this scheme does not appear to be practical. An alternate approach to the data processing problem is presented next.

Rapp² gives the transformation that connects north, east, and vertical at a given longitude and latitude with Earth Centered Earth Fixed x , y , z ; this is shown as Equation (10) below. The x_k , y_k , and z_k are observations of the vector baseline components obtained from GPS and corrected for the local deflections of the vertical. If we admit that no matter how careful we are positioning the baseline normal to the geoid, there will always be small errors in the east and north directions whose components are n_b and e_b . These might be accounted for if they are treated as bias parameters that must be included in the position solution. From each baseline solution, there are three observations (x_k , y_k , and z_k) to be used on the left-hand side of Equation (10). There are five unknowns (λ , ϕ , n_b , e_b , and u_b) on the right-hand side. Therefore, at a given site there must be k sets of observations from different satellite geometries that give k independent baseline determinations for the components x_k , y_k , and z_k . For each baseline solution, there are $3k$ observations and 5 unknowns. When $k \geq 2$ the number of observations equals or exceeds the number of unknowns and a solution for longitude, latitude, and the biases should be possible.

$$\begin{aligned}x_k &= -(\sin\phi\cos\lambda) n_b -(\sin\lambda) e_b +(\cos\phi\cos\lambda) u_b \\y_k &= -(\sin\phi\sin\lambda) n_b +(\cos\lambda) e_b +(\cos\phi\sin\lambda) u_b \\z_k &= (\cos\phi) n_b +(\sin\phi) u_b\end{aligned}\tag{10}$$

An initial guess for λ and ϕ can be obtained from the SPS position solution. With the baseline approximately normal to the ellipsoid, the initial guess for n_b and e_b is zero and for u_b is the measured baseline length. A least squares solution including two or more observations of the baseline vector may be able to improve on the initial estimate of λ and ϕ . Ultimately, the accuracy of the method will depend upon the knowledge of the local vertical deflections.

POINTING AND RANGING TO A KNOWN LANDMARK

If a GPS survey is desired in a localized area that has one or more precisely known absolute references, it would be possible to use a single receiver of the direction-finding type along with an electronic distance measuring device to locate points in line-of-sight to the references. A more accurate way to perform the same task (with two receivers) would be to locate one GPS receiver over the reference point and another successively over the unknown

points. If this were not possible for some reason or if only a single direction-finding receiver were available, the survey could be performed, but with lower accuracy than with two independent receivers. This method is the inverse of that described by O'Leary, Evans and Smith.³

Figure 4 illustrates the geometry that the method requires. The reference point is located by the known WGS84 vector, r_R , and is indicated by the solid dot. The point to be determined is indicated by the $+$. The unit vector from the unknown point to the reference point is determined by aiming a theodolite-like device at the reference point. The theodolite would include a short GPS baseline positioned over the unknown point. The range R to the reference point is obtained from a laser rangefinder. Errors in the measurements are represented by ΔR and $\Delta\theta$ in Figure 4. O'Leary concluded that the angular error introduced 1 m of error per kilometer of range (2-m GPS baseline). The range error was found to be about 5 m for noncooperative targets up to a limiting range of a few kilometers. A noncooperative target implies that no laser retroreflector was used.

POINTING TO A STELLAR OBJECT

This technique depends entirely upon angular measurements; therefore, several sightings to stellar objects are required for good results. The method is similar to that exploited by the sextant, but instead of measuring the elevation of an object above the local horizon,⁴ the three-dimensional unit vector to that object is determined. The theodolite-like device equipped with a short GPS baseline is aligned with the stellar object. Real time GPS attitude algorithms can be used to obtain the instantaneous unit vector.

With several unit vectors to known stellar objects found, a least squares fit to the data can be used to determine absolute position. Assuming precise alignment of the optical axis with the GPS baseline, the accuracy of the result would depend upon transverse baseline error. If that error were about 1 mm, then the angular error for a 1-m baseline would be about 1 mrad. The results would be similar to those described in the next section with the exception that attitude-determining GPS receivers could be used unmodified and with current algorithms to determine the unit vectors. Additional work would be necessary to integrate these algorithms with the stellar data and with the final absolute positioning routine.

INTERFEROMETRIC GPS OBSERVATIONS

Standard GPS relative positioning techniques are sometimes referred to as interferometry. Classic interferometry implies that the array of antennas form an array reception pattern by

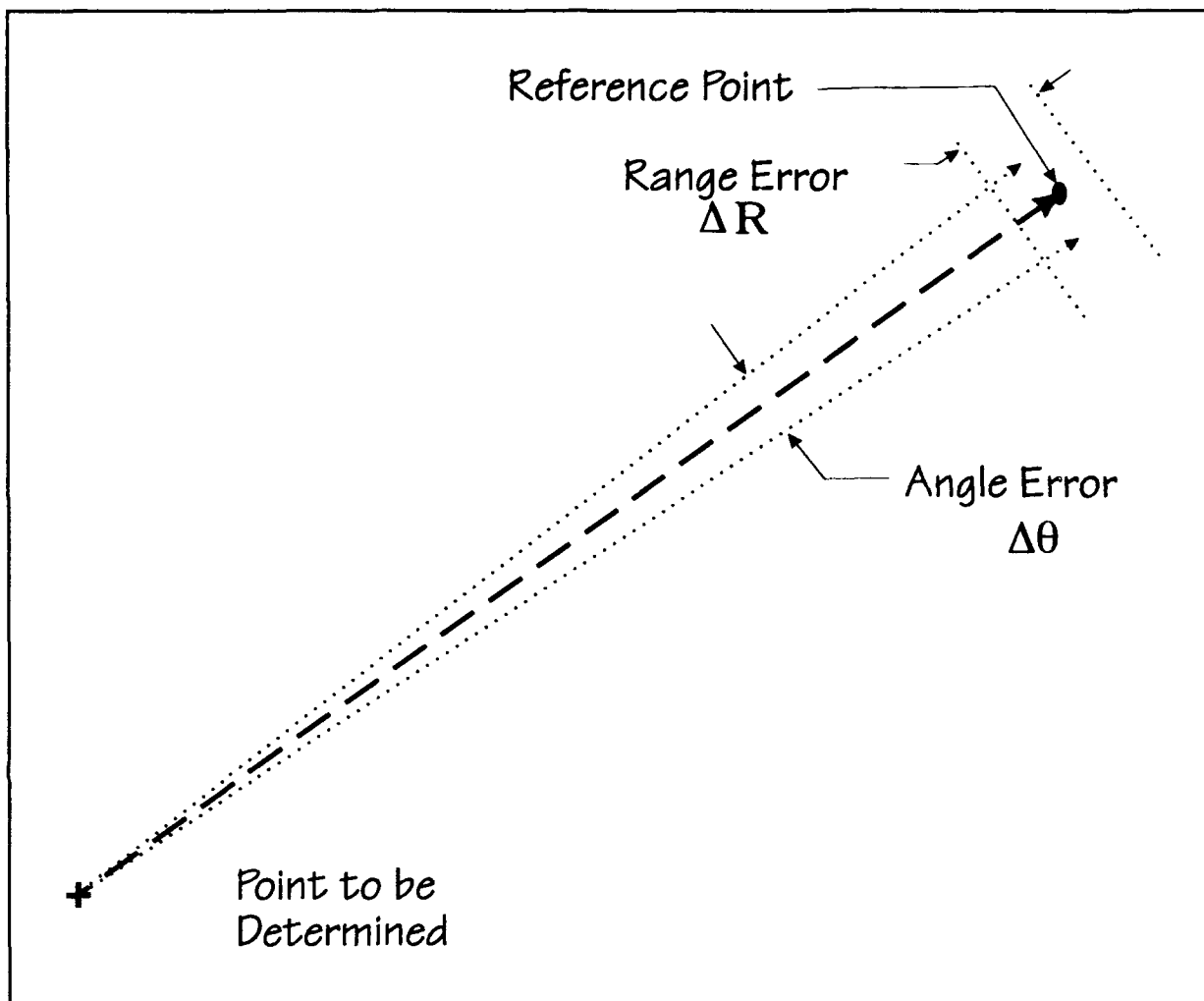


FIGURE 4. GPS AND RANGE-FINDING TECHNIQUE

adding or multiplying the antenna signals together before processing. In standard GPS relative positioning, the observations from each antenna are treated independently and incoherently. The Doppler phase counts are referenced to the receiver's local frequency standard and the numeric phase differences are recorded at regular intervals. In interferometry, the received *radio frequency* phases are added directly so that they interfere and form the array pattern (sometimes referred to as fringes) shown in Figure 5. The geometry for the array pattern formed by a two-element interferometer is illustrated in Figure 6. The interference pattern can be recreated numerically if the processing is coherent. This is accomplished if the baselines are short and a common local frequency standard is used as the reference for all phase data.

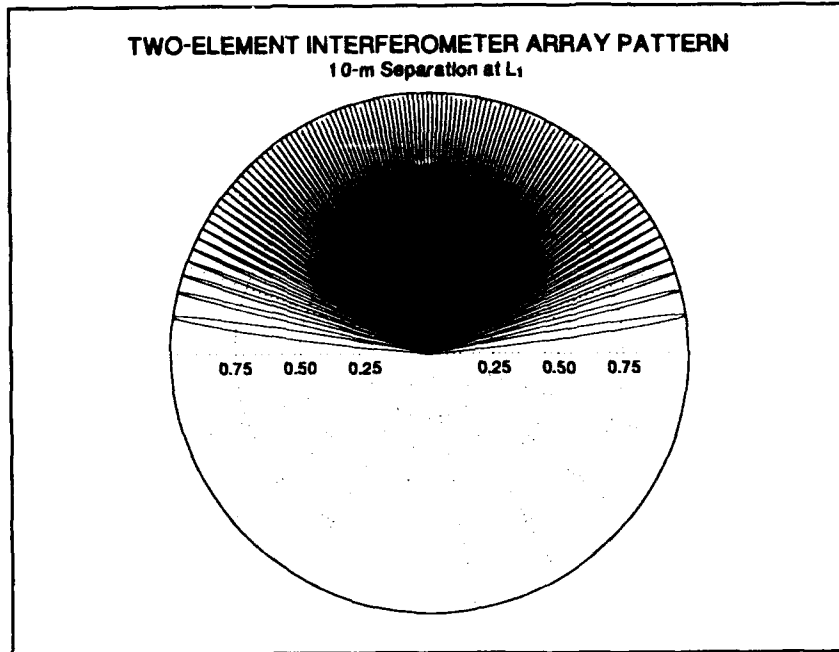


FIGURE 5. TWO-ELEMENT INTERFEROMETER ARRAY PATTERN

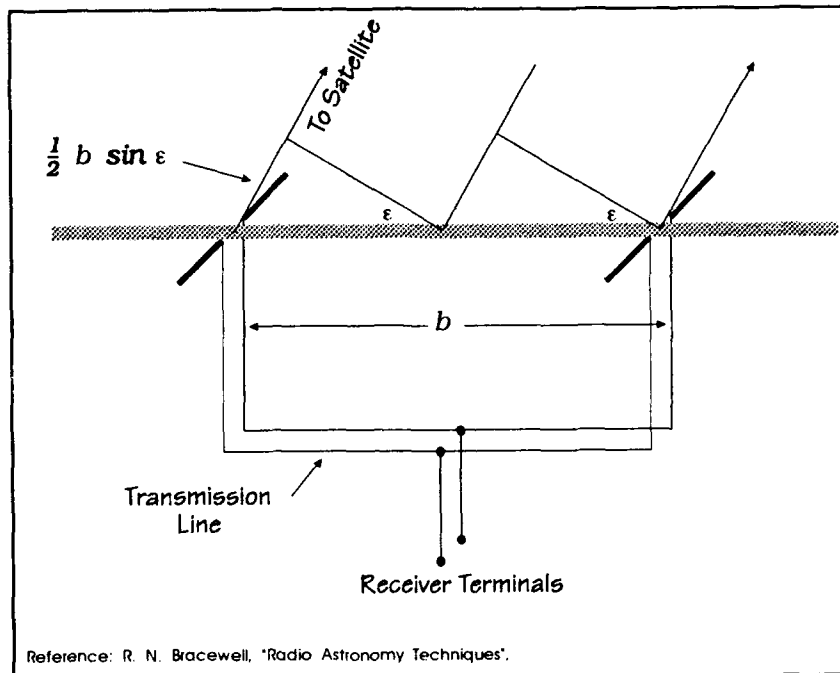


FIGURE 6. TWO-ELEMENT INTERFEROMETER ANTENNA ARRAY

Given a fixed baseline defined by the phase centers of two antennas, the array pattern is fixed to and rotates with the earth. The GPS satellites will pass through the fringes as they pass overhead. If the signals from the two antennas shown in Figure 6 were connected to a normal GPS receiver, it could track the satellites in the usual way with the exception that the antenna pattern has peaks and nulls rather than being omnidirectional. If the receiver has an accurate way to record signal strength these observations of signal strength for each satellite over a period of time would be enough to fix it in a particular track through the sky. Since the satellite positions are known, the direction of the baseline determined in the usual relative positioning mode and the satellite tracks in the sky should be enough to isolate the location of the observer. The accuracy with which this could be accomplished depends upon the null-to-null spacing of the array pattern.

$$D_i(\epsilon) = 1 + \cos\left(\frac{2\pi b \sin\epsilon}{\lambda}\right) \quad (11)$$

From the equation for the array pattern [Equation (11)], the change $\Delta\epsilon$ of elevation angle ϵ for one cycle of interference when $\epsilon \approx \pi/2$ is approximately λ/b . In the case where b is 100 m, the fringe spacing is about 0.002 rad at L_1 . Figure 5 illustrated the fringe pattern as a function of ϵ for a baseline of 10 m. Notice that the spacing varies according to the *sine* of ϵ and is coarse at the horizon and fine at the zenith. The variation may give some additional information about the elevation angle of the satellites.

As with the other schemes outlined above, the short distance between antennas limits the angular precision and consequently the accuracy of the derived absolute position. In the example, the 2-mrad fringe spacing that results from a 100-m baseline corresponds to a distance of 40 km at GPS altitudes. If observations over a period of time can subdivide the null to null angle into 1000 parts, the satellite position can still be in error by about 40 m. This is on the order of the error introduced by SA-epsilon and, without further analysis, seems to offer little if any improvement in the absolute position one would obtain with the conventional SPS techniques.

MINIMIZING THE RESIDUAL OF FIT

When performing relative positioning solutions, the satellite ephemeris and an estimate of the absolute position of the reference antenna is required to compute P_{sjk} in Equation (2). A plane geometrical representation is presented in Figure 7. For each antenna pair, the observation is the time difference of arrival (l) of the wavefront between the two antennas. This can be expressed as a function of the baseline b , the range r , and the elevation angle ϵ of the satellite as seen from the reference antenna. The expression for l in length units is shown in Equation (12).

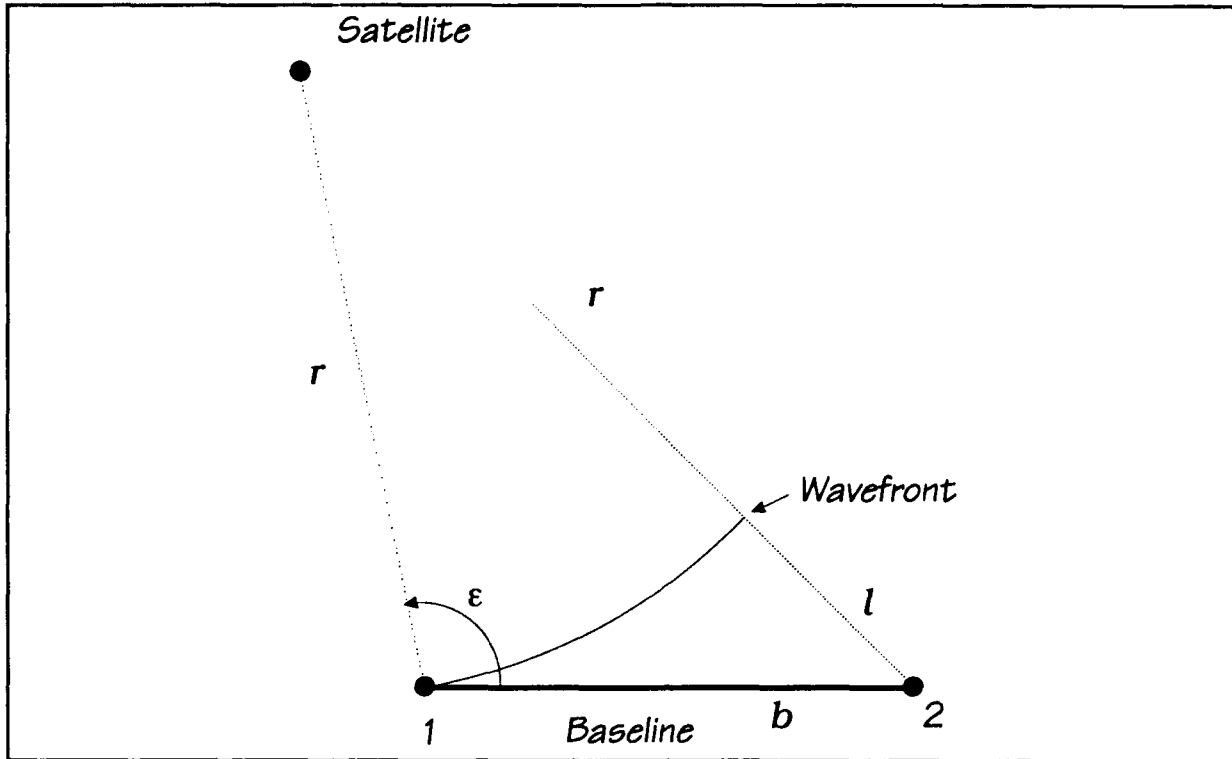


FIGURE 7. RELATIVE POSITIONING GEOMETRY

$$l = \sqrt{r^2 + b^2 - r b \cos \epsilon} - r \quad (12)$$

A translational shift in the location of the reference antenna or the satellite will produce a change in the elevation angle. The sensitivity of ϵ to a change in l is given by the partial derivative in Equation (13). For the case of GPS positioning a point on the earth, the range $r \gg b$ and the partial can be approximated by Equation (14).

$$\frac{\partial l}{\partial \epsilon} = \frac{\frac{1}{2} r b \sin \epsilon}{\sqrt{r^2 + b^2 - r b \cos \epsilon}} \quad (13)$$

$$\frac{\partial l}{\partial \epsilon} \approx \frac{1}{2} b \sin \epsilon \quad (14)$$

Assuming the satellite position is known through its ephemeris, a small horizontal displacement in the baseline Δs will cause a change in the elevation angle of approximately $\Delta s/r$ (for $\epsilon \approx 90$ deg). This in turn leads to a change in l given by Equation (15).

$$\Delta l = \left(\frac{b}{2} \sin \epsilon \right) \frac{\Delta s}{r} \quad (15)$$

With $\epsilon \approx 90$ deg, $r \approx 2 \times 10^8$ m, and $b \approx 30$ m, the evaluation of Equation (15) returns the expression given in Equation (16).

$$\Delta l = 7.5 \times 10^{-8} \Delta s \quad (16)$$

If the minimum detectable Δl is 1 mm, then the expected sensitivity to an error in absolute position is about 13.3 km.

MULTIPLE BASELINE EXPERIMENT

An experiment to investigate the potential of the technique above was performed in January 1993 at NSWCDD. A direction-finding receiver was used with four antennas. The particular receiver used had 24 satellite channels that were allocated in four banks of six L₁ trackers. The antennas were connected to the receiver through 30-m cables. Thus, with the receiver in the center of a square, the opposite corners can be up to 60 m apart. Since the four banks of trackers originate from the same receiver, there is no time or frequency deviation between them. Therefore, the standard double-difference would not be required; a single-difference between satellite measurements should suffice. A diagram of the experimental layout is shown in Figure 8.

Two consecutive days of data were collected at the site. The time interval between observations was selected to be 20 sec. The distribution of satellites on 14 January 1993 was as depicted in Figure 9. The elevation angle below which no data were accepted was set to 12 deg. The on-line receiver software selected and automatically tracked the same set of satellites at each antenna. The data were recorded internally and were downloaded once each day. The standard double-difference software uses a single-reference satellite for each solution. When the solution

is performed, the user has the option of choosing which satellite should be the reference, the identity of the other satellites included, and the number of observation epochs to process.

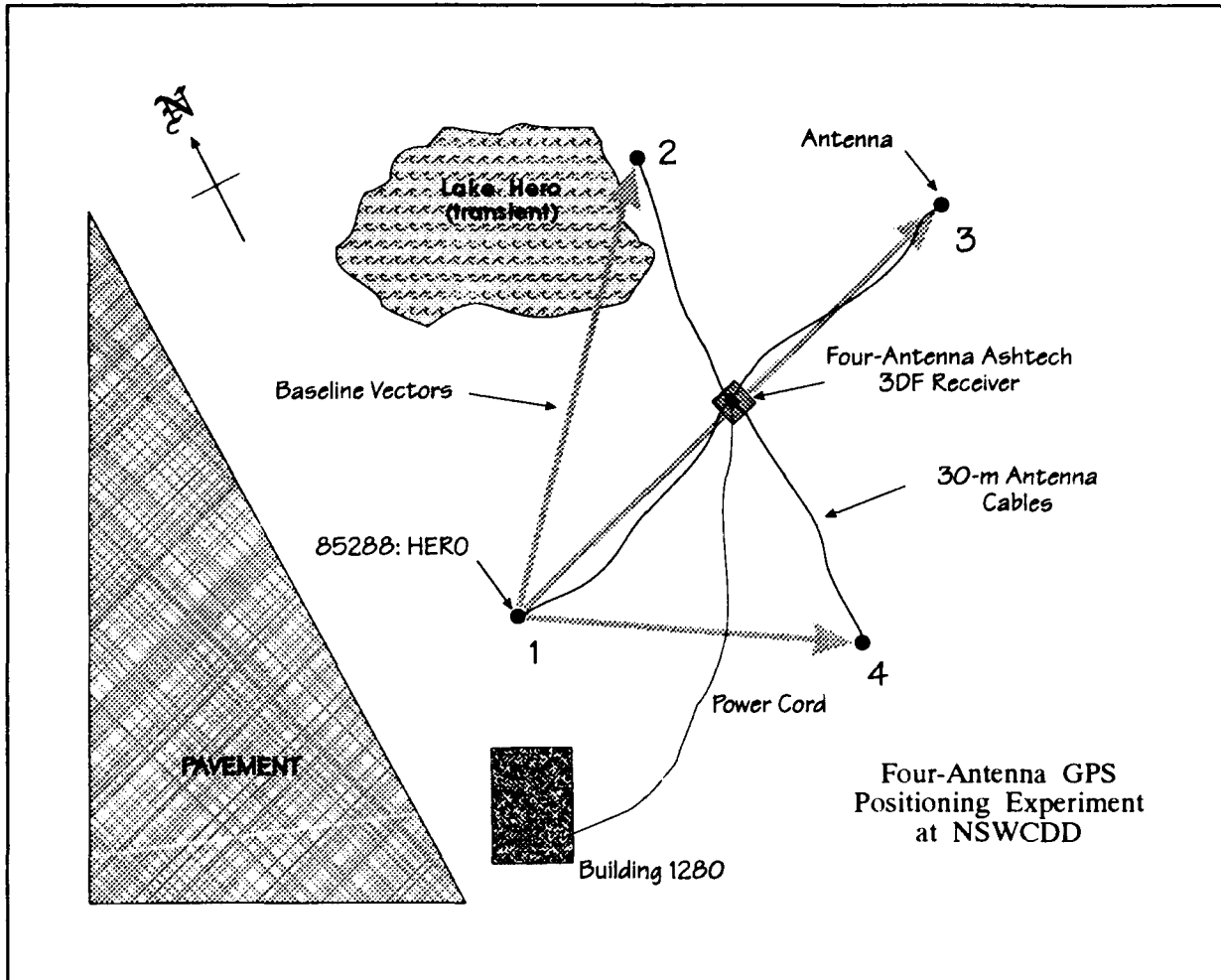


FIGURE 8. FOUR-ANTENNA ARRAY AT THE HERO SITE AT NSWCDD: 14-15 JANUARY 1993

To illustrate the repeatability of the solutions, six different time spans (partially overlapping) with different reference satellites were processed each day. The 12 solutions for each baseline are listed in the Tables 1 through 3. Figures 10 through 12 show the scatter in the solutions listed in the tables. One of the trackers in the fourth bank of six channels suffered from an excessive number of unexplained phase jumps. Therefore, the satellites tracked by this channel were omitted from the solutions. As a result, some of the baselines were not as well determined

as they could have been had the data from those satellites been processed. Even with the bad satellite channel, the baselines were repeatability determined at the millimeter level.

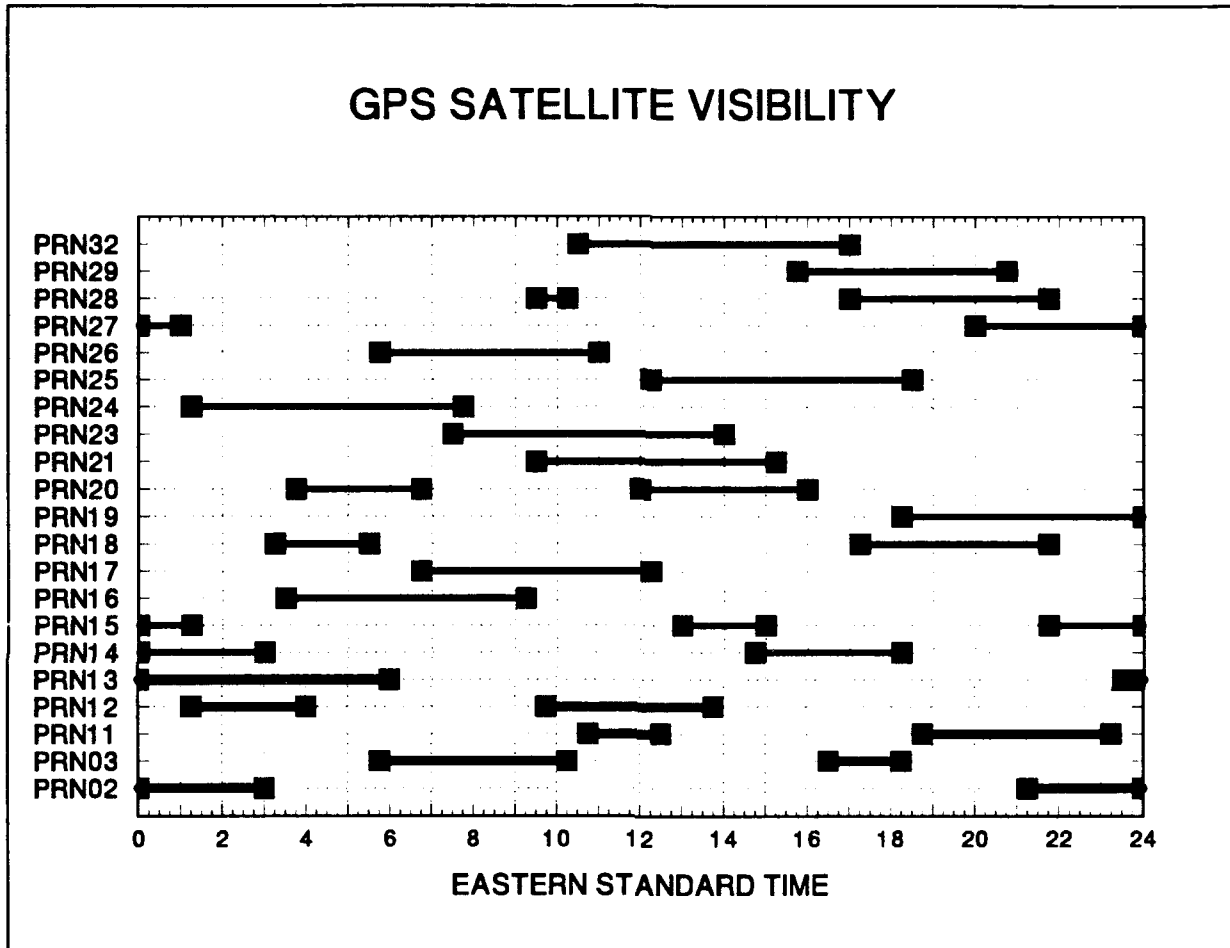


FIGURE 9. SATELLITES VISIBLE AT NSWCDD ON 14 JANUARY 1993

Table 1 lists the results for the 12 solutions computed for baseline 1-2. The leftmost column lists the day and the second column shows the reference satellite used for that solution. The next three columns are the x , y , z components of the baseline vector followed by its length. The rightmost column lists the residual for the double-difference fit. The average residual was found to be 3.010 mm with a standard deviation of 0.220 mm. The residual was a little larger than the 1.9-mm standard deviation on the baseline length. Tables 2 and 3 show similar results for baselines 1-3 and 1-4, respectively. The average residual for baseline 1-3 was 3.088 mm and for baseline 1-4 it was 3.083 mm.

The root-mean-square (rms) of the residuals, however, were consistently between 2 and 4 mm. The residual plots show that this rather high rms is due to systematic variations that are not attributable to system noise. These *signals* may be due to multipath effects, some environmental condition, or a propagation effect that repeats from day to day. Examples of the summary residual plots for each baseline and each satellite pair on day 015, with PRN 19 as the reference satellite, are shown in Figures 12 through 15. A comparison from one day to the next for one satellite pair (PRN 11-19) is illustrated in Figures 16 and 17. Notice how well this residual is repeated on the second day; this signature is typical of multipath. However, it does not explain why the other satellite's residuals in the summary plots are so similar to the PRN 11-19 residual. Though all the residuals in Figure 14 have PRN 19 in common, it is surprising that the similarity is so strong. Similar comments can be made about the baseline-to-baseline correlations.

For this demonstration, repeated relative positioning solutions were performed keeping all variables the same except for the given site position. This mimics having the site position unknown and letting the rms of the relative positioning solution be the indicator of the true position. The lower the residual of the fit, the smaller the model error due to position error. Given many starting positions (each one offset a different amount from the correct value), the rms of the residual should indicate a minimum value near the true location. This is verified by the results for longitude shown in Figure 18 and for latitude shown in Figure 19. In each case, the minimum is too shallow to accurately determine the true location to better than about 1 km. Accuracies on the order of 10 m would require lengthening the baselines by a factor of 100. The 30 m baselines would need to become 3 km or greater. Short baselines have the advantage that real-time solutions could be obtained on the spot. When receivers are separated by a few kilometers, a communication link would need to be employed. Near real-time precise relative positioning software has become available for baselines up to 50 km.

TABLE 1. SOLUTIONS FOR BASELINE 1 - 2

Day	Reference Satellite	X(m)	Y(m)	Z(m)	L(m)	Residual (mm)
014	13	20.8746	30.1871	31.5376	48.3904	2.656
014	19	20.8740	30.1881	31.5383	48.3912	2.866
014	23	20.8735	30.1889	31.5375	48.3909	2.941
014	24	20.8745	30.1876	31.5375	48.3906	2.878
014	25	20.8746	30.1874	31.5380	48.3909	3.071
014	32	20.8734	30.1885	31.5365	48.3900	3.032
015	13	20.8741	30.1855	31.5385	48.3898	3.232
015	19	20.8734	30.1875	31.5391	48.3911	2.890
015	23	20.8740	30.1885	31.5385	48.3915	2.730
015	24	20.8740	30.1856	31.5394	48.3904	3.218
015	25	20.8742	30.1867	31.5395	48.3912	3.278
015	32	20.8736	30.1869	31.5392	48.3909	3.326
Average		20.8740	30.1874	31.5383	48.3907	3.010
Standard Deviation		0.0004	0.0011	0.0009	0.0005	0.220

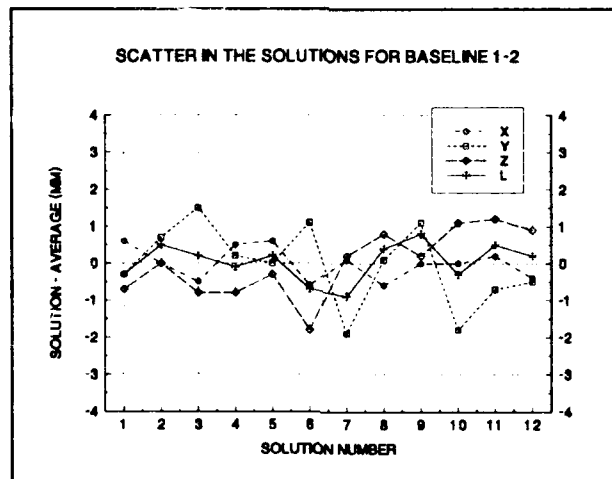


FIGURE 10. RESULTS OF TABLE 1 PLOTTED

TABLE 2. SOLUTIONS FOR BASELINE 1 - 3

Day	Reference Satellite	X(m)	Y(m)	Z(m)	L(m)	Residual (mm)
014	13	48.8642	25.8395	18.1896	58.1915	2.913
014	19	48.8640	25.8406	18.1898	58.1919	2.833
014	23	48.8636	25.8413	18.1903	58.1920	2.947
014	24	48.8638	25.8400	18.1895	58.1914	3.051
014	25	48.8642	25.8396	18.1895	58.1915	3.066
014	32	48.8635	25.8411	18.1895	58.1916	3.266
015	13	48.8637	25.8374	18.1913	58.1907	3.274
015	19	48.8632	25.8403	18.1909	58.1914	2.677
015	23	48.8629	25.8412	18.1906	58.1915	2.734
015	24	48.8630	25.8378	18.1916	58.1904	3.291
015	25	48.8637	25.8395	18.1917	58.1918	3.581
015	32	48.8629	25.8396	18.1917	58.1911	3.419
Average		48.8636	25.8398	18.1905	58.1914	3.088
Standard Deviation		0.0005	0.0012	0.0009	0.0005	0.282

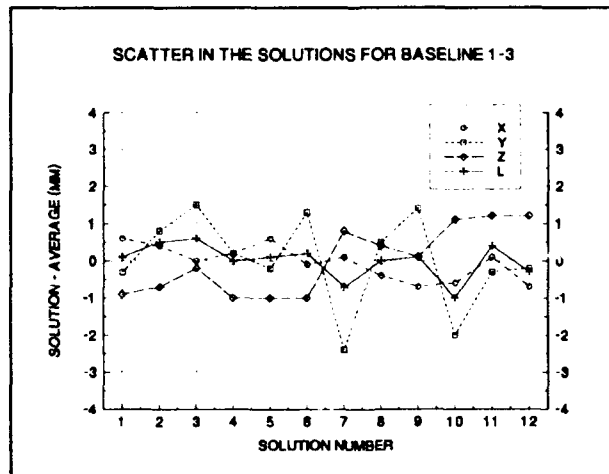


FIGURE 11. RESULTS OF TABLE 2 PLOTTED

TABLE 3. SOLUTIONS FOR BASELINE 1 - 4

Day	Reference Satellite	X(m)	Y(m)	Z(m)	L(m)	Residual (mm)
014	13	30.8107	-4.3793	-14.1850	34.2007	2.607
014	19	30.8110	-4.3746	-14.1859	34.2008	4.145
014	23	30.8096	-4.3763	-14.1865	34.2000	2.817
014	24	30.8107	-4.3798	-14.1845	34.2007	2.734
014	25	30.8090	-4.3774	-14.1821	34.1978	3.770
014	32	30.8093	-4.3774	-14.1869	34.2000	3.184
015	13	30.8098	-4.3803	-14.1835	34.1995	2.870
015	19	30.8088	-4.3779	-14.1850	34.1989	2.818
015	23	30.8099	-4.3773	-14.1852	34.1998	2.760
015	24	30.8098	-4.3804	-14.1831	34.1993	2.904
015	25	30.8096	-4.3803	-14.1835	34.1993	3.329
015	32	30.8094	-4.3789	-14.1841	34.1992	3.057
Average		30.8098	-4.3783	-14.1846	34.1997	3.083
Standard Deviation		0.0007	0.0018	0.0014	0.0009	0.461

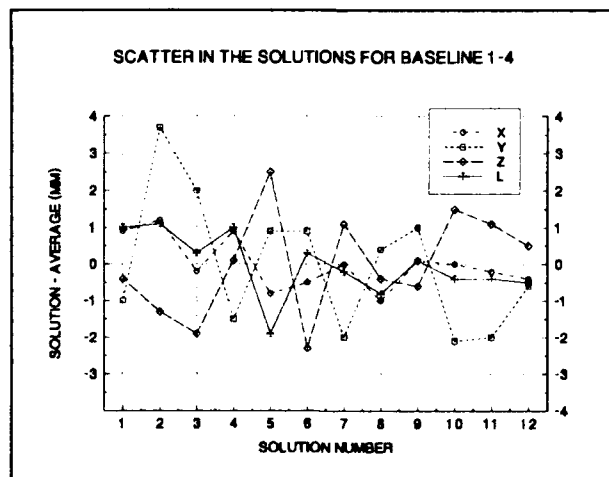


FIGURE 12. RESULTS OF TABLE 3 PLOTTED

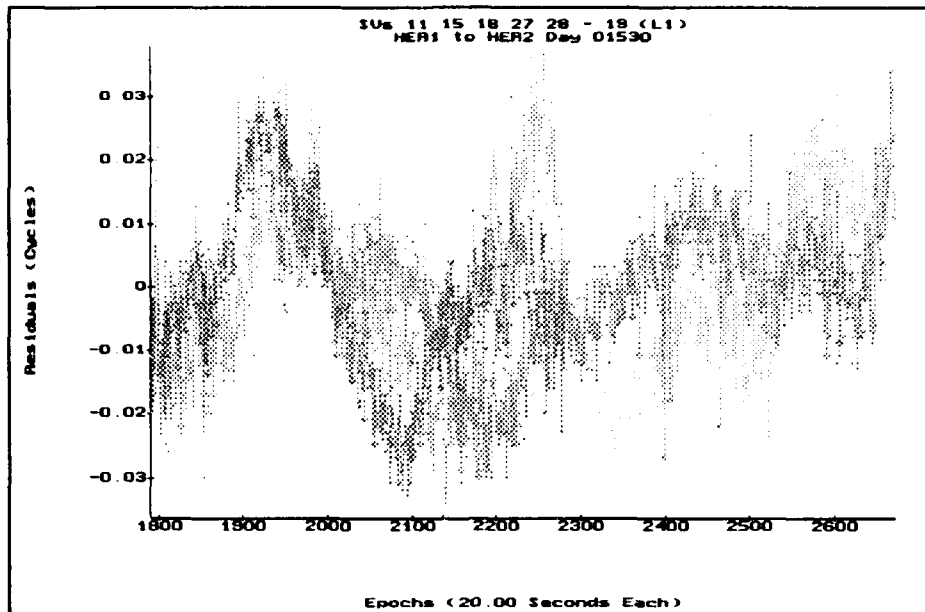


FIGURE 13. SUMMARY PLOT FOR BASELINE 1-2 ON DAY 015 WITH PRN 19 AS REFERENCE

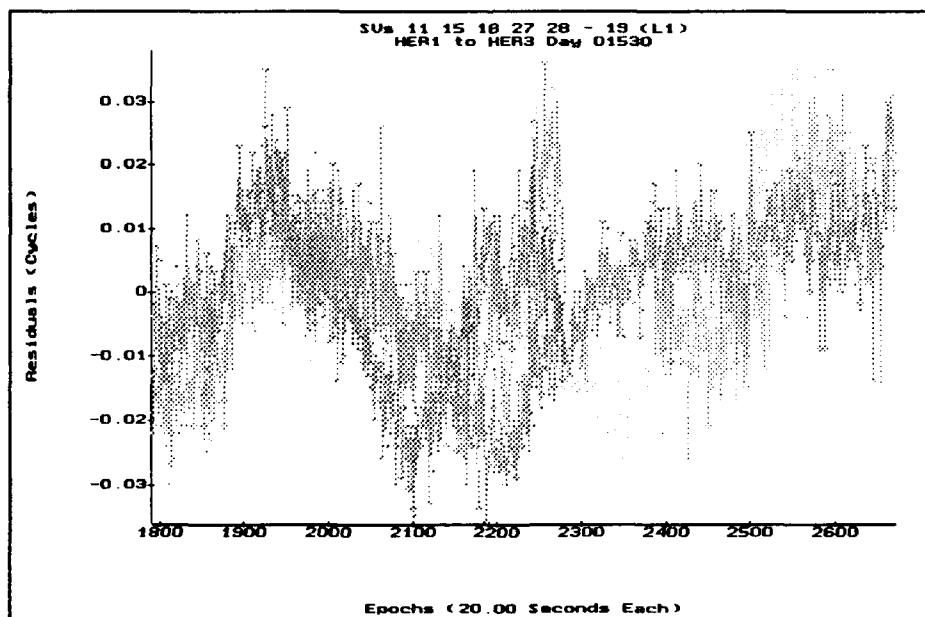


FIGURE 14. SUMMARY PLOT FOR BASELINE 1-3 ON DAY 015 WITH PRN 19 AS REFERENCE

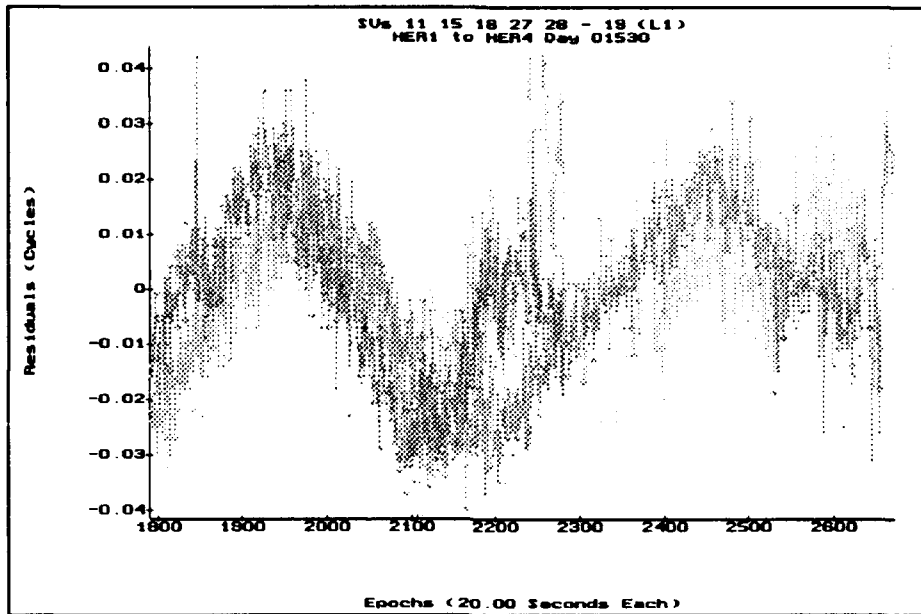


FIGURE 15. SUMMARY PLOT FOR BASELINE 1-4 ON DAY 015 WITH PRN 19 AS REFERENCE

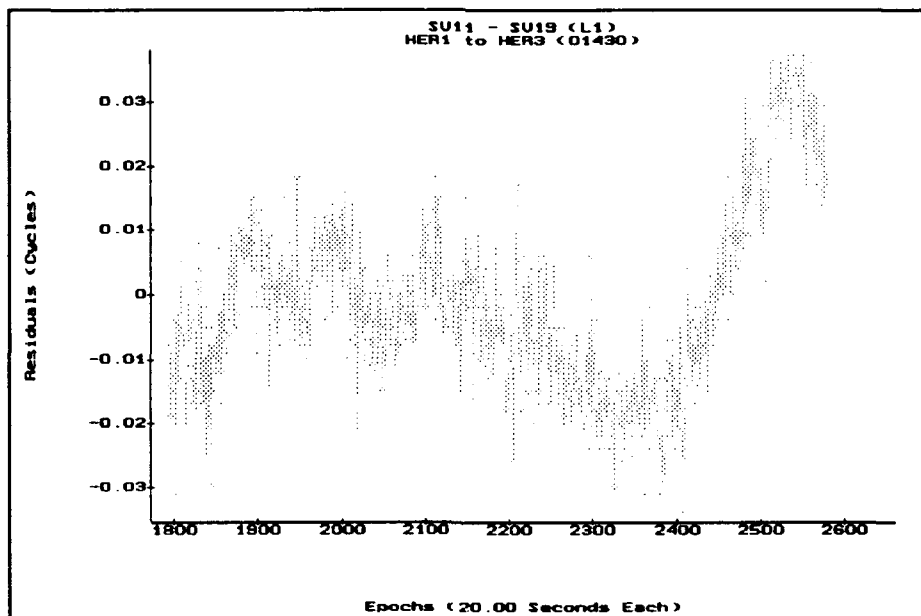


FIGURE 16. SATELLITE PAIR 11-19 DOUBLE-DIFFERENCE RESIDUAL FROM BASELINE 1-3 ON DAY 014

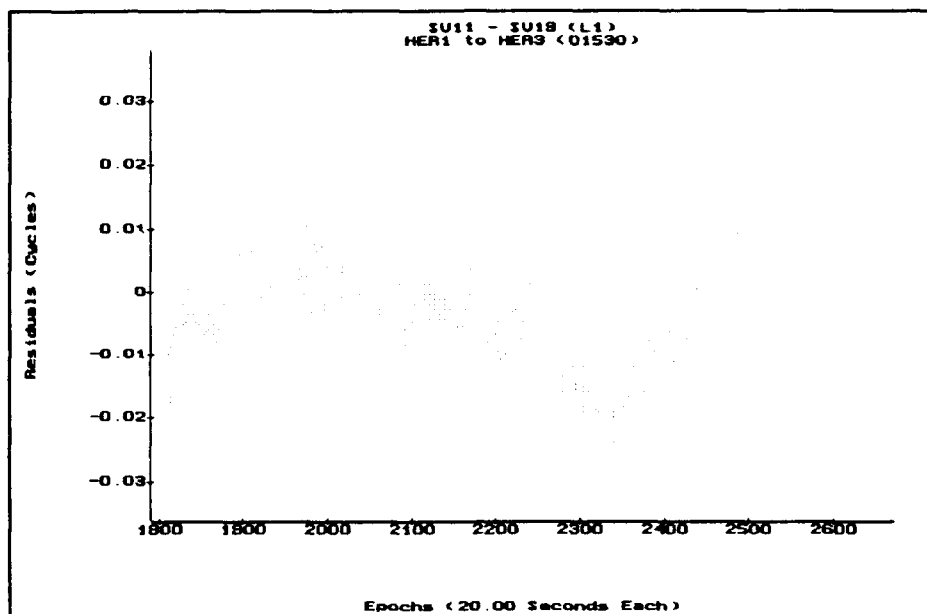


FIGURE 17. SATELLITE PAIR 11-19 DOUBLE-DIFFERENCE RESIDUAL FROM BASELINE 1-3 ON DAY 015

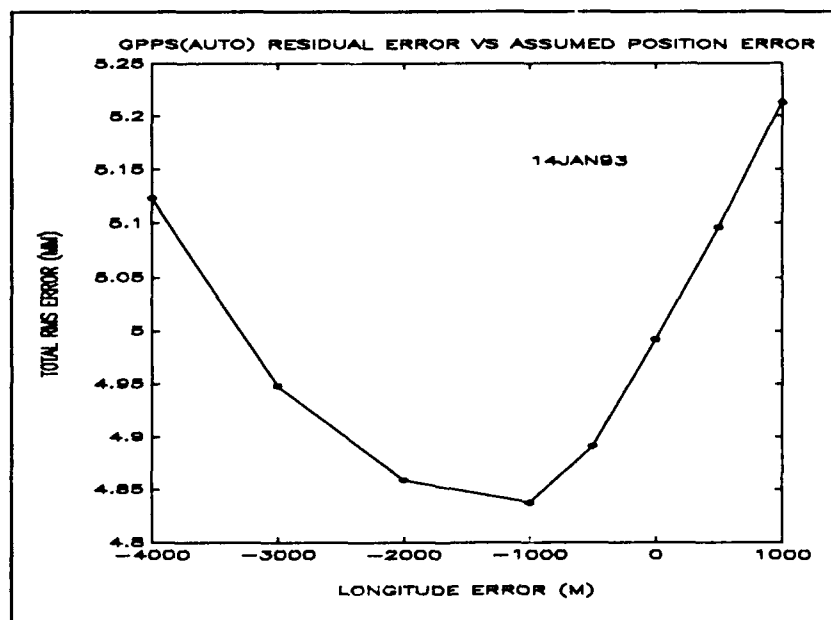


FIGURE 18. DOUBLE-DIFFERENCE RMS RESIDUAL FOR LONGITUDE OFFSETS

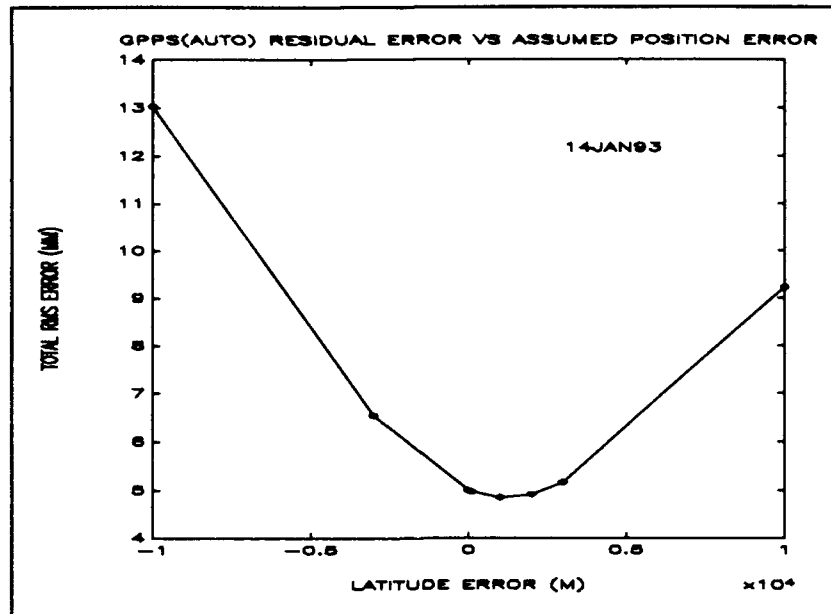


FIGURE 19. DOUBLE DIFFERENCE RMS RESIDUAL FOR LATITUDE OFFSETS

GPS AND LEVELING

The objective of this procedure is to obtain a vector normal to the ellipsoid at the reference site. This vector defines the latitude and longitude at the site. The procedure to estimate the vector components is given below and is demonstrated using data collected during a test at NSWCDD in 1987.

The procedure involves collecting both GPS and first-order leveling data along two baselines radiating from the reference site and, preferably, separated by an angle of about 90 deg. Using an assumed initial value of position, the baseline vector (defining Δx , Δy , and Δz) is determined using standard GPS relative positioning techniques. These vector values have been found to be somewhat insensitive to the initially assumed position for the baseline lengths discussed here. Use of the C/A-determined initial position is adequate. The baseline length, heights (h_1 and h_2) above the ellipsoid, and azimuth are then obtained. In addition, first-order leveling difference in height is obtained (ΔH) and values of deflection of the vertical (ξ and η) are obtained using a gravitational model. The deflection in the baseline direction is⁵

$$\epsilon = (\cos \alpha) \xi + (\sin \alpha) \eta \quad (17)$$

where

- α = geodetic azimuth
- ξ = north-south component of vertical deflection
- η = east-west component of vertical deflection

The height correction to h_2 for the deflection ϵ is given by Equation (18), where Δs is the baseline length.

$$\Delta h_\epsilon = -\epsilon \Delta s \quad (18)$$

The leveling ΔH and vertical deflections Δh_ϵ corrections are made to the height h_2 . If the geoid and the ellipsoid model did not curve, these would be the only corrections needed to obtain the tangent vector to the ellipsoid. However, a curvature correction is required as illustrated in Figure 20. An approximate geometric correction is given by the following expressions where R_E is the radius of the earth.

$$\theta = \frac{\Delta s}{R_E} \quad (19)$$

$$\Delta h_c \approx \frac{R_E}{\cos \theta} - R_E$$

$$\hat{h}_{TAN2} = h_2 - \Delta H - \Delta h_\epsilon + \Delta h_c \quad (20)$$

The position of the tangent vector can now be described by Equation (20) and the original latitude and longitude by ϕ_2, λ_2 . These values are converted to earth-fixed orthogonal coordinates of x_2, y_2 and z_2 and differenced with the reference site values to obtain the ellipsoid tangent vector defined as v_{x1}, v_{y1} , and v_{z1} . Next, a second tangent vector is obtained by the above procedure for a baseline from the reference site and, preferably, roughly perpendicular to the first baseline. The second vector is defined as v_{x2}, v_{y2} , and v_{z2} . The cross product is given by the vector w whose components are expanded in Equations (21) and (22). The corresponding unit vector components are found using Equation (22).

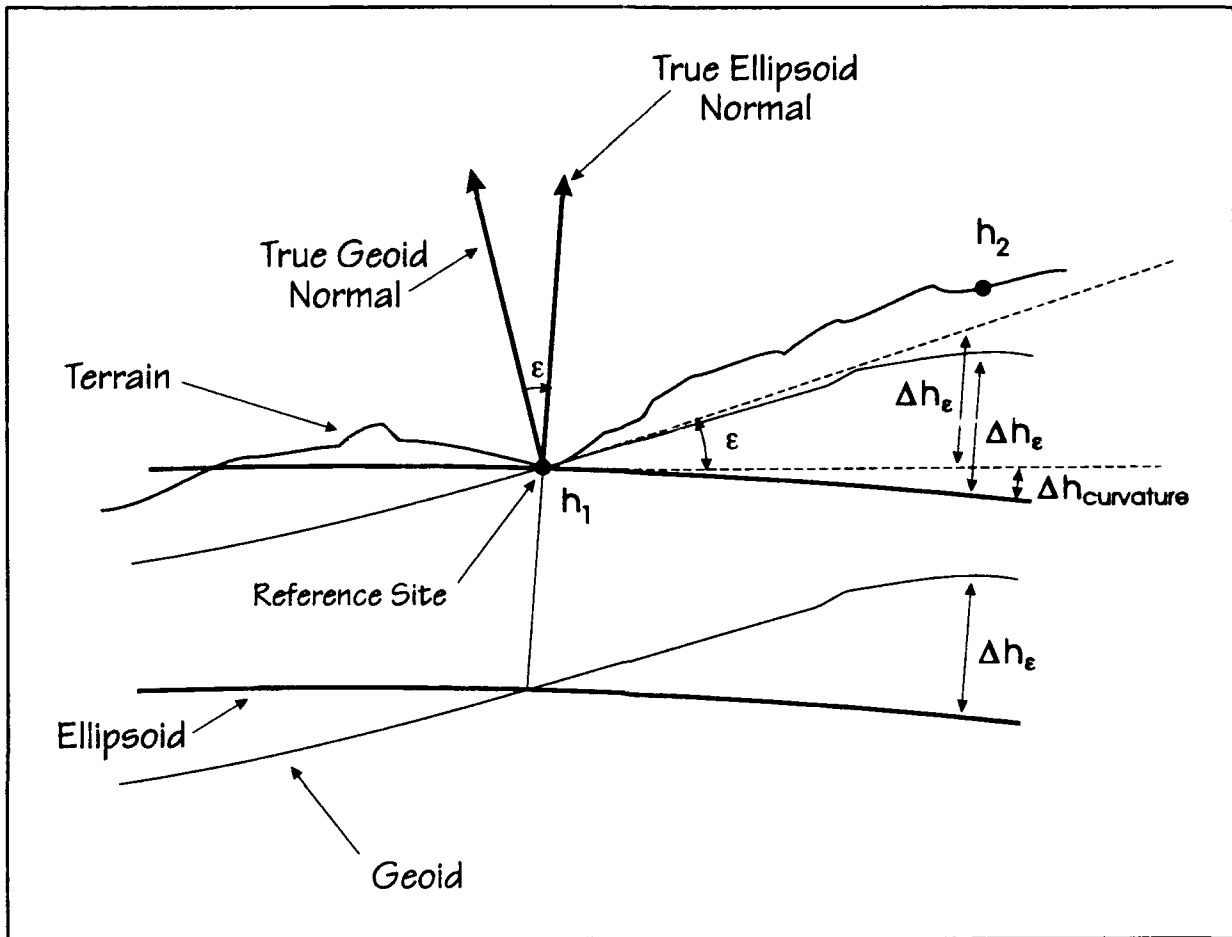


FIGURE 20. DIAGRAM OF HEIGHT CORRECTIONS FOR OBTAINING THE TANGENT TO THE ELLIPSOID AT THE REFERENCE POSITION

$$\begin{aligned}
 w_1 &= v_{y1}v_{z2} - v_{y2}v_{z1} \\
 w_2 &= v_{x2}v_{z1} - v_{x1}v_{z2} \\
 w_3 &= v_{x1}v_{y2} - v_{x2}v_{y1}
 \end{aligned}
 \tag{21}$$

$$u_i = \frac{w_i}{|w|}
 \tag{22}$$

The last step of the procedure is to obtain the estimated latitude and longitude ($\hat{\phi}_1$ and $\hat{\lambda}_1$) from the normal unit vector relationship given in Equation (7). Explicitly this is given in Equation (23).

$$\begin{aligned}\hat{\phi}_1 &= \arcsin(u_3) \\ \hat{\lambda}_1 &= \arctan\left(\frac{u_2}{u_1}\right)\end{aligned}\tag{23}$$

The positioning procedure has been demonstrated and validated using test data taken in 1987 at NSWCDD.⁶ The GPS baselines and the leveling loop are presented in Figure 21.⁷ For the current demonstration, only two baselines were analyzed; these are from site MBRE to BOM2 and MBRE to CHUR. At the reference site (MBRE), astrogeodetic vertical deflection measurements were also obtained by the U S Naval Observatory (USNO). Two and three days of GPS data were collected at the above baselines, respectively, using TI4100 receivers. These data were processed using the National Geodetic Survey (NGS) PHASER software and DMA/NSWCDD post-fit precise ephemerides. The vector values, the baseline length, and the azimuth from the GPS solutions are given in Table 4; also given are the first-order leveling height differences.

TABLE 4. RESULTS FROM THE TEST AT NSWCDD

Vector Values	BASELINE	
	MBRE to BOM2	MBRE to CHUR
Δx (m)	464.891	-4668.231
Δy (m)	2318.125	-368.816
Δz (m)	2720.982	913.228
Δs (m)	3640.660	4770.995
$\Delta \alpha$ (m)	15.667219	283.866708
ΔH (m)	-1.8364	27.7834

The demonstration analyses consists of two cases. The normal to the ellipsoid vector is found with and without a qualified position offset. The position offset must be qualified, since it was not used for both the solutions of the baseline vector Δx , Δy , and Δz or for the modeled

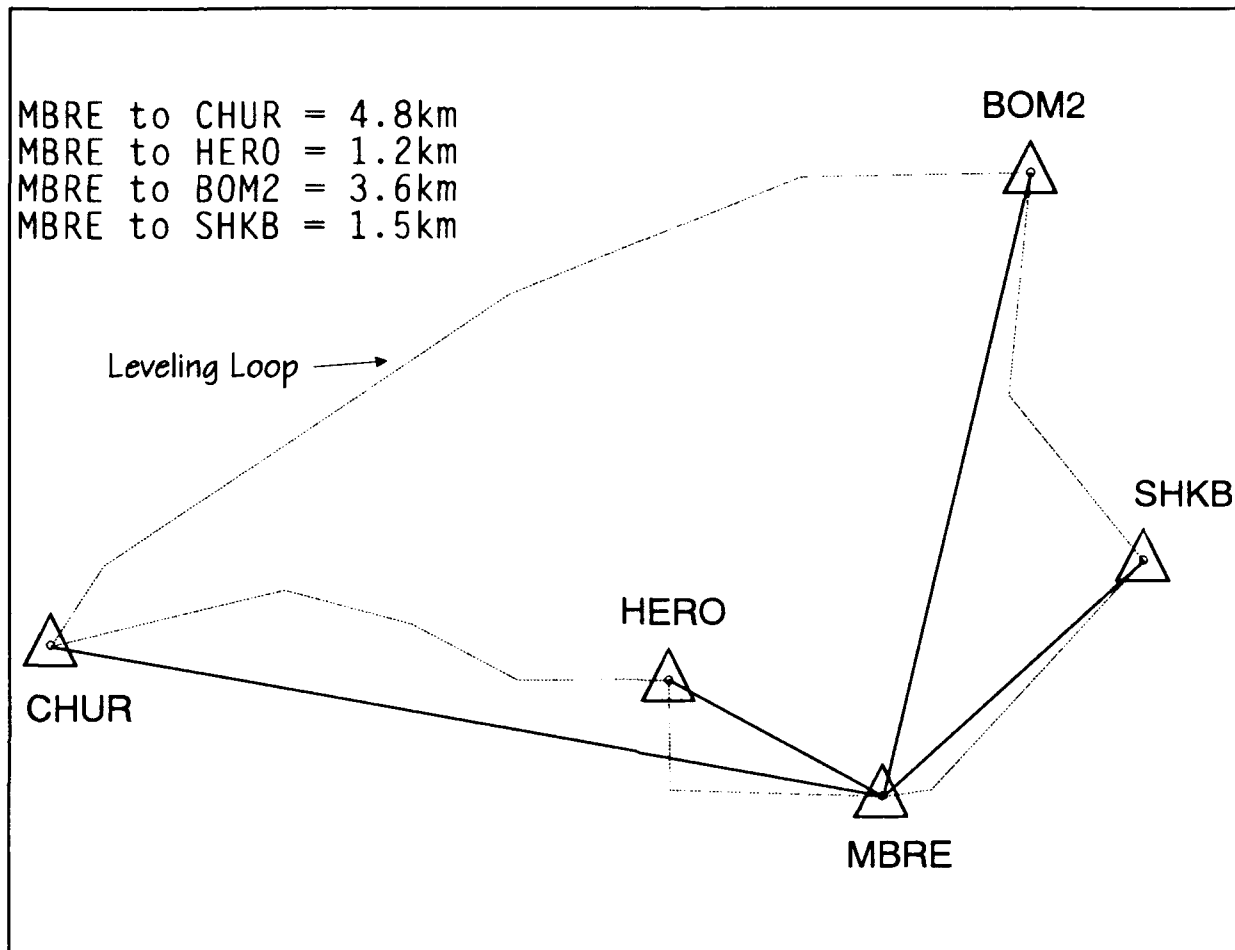


FIGURE 21. GPS BASELINES AND LEVELING LOOP

vertical deflection values; these are both insensitive to assumed position. The modeled vertical deflection values ($\xi = -2.89$ arcsec and $\eta = 4.79$ arcsec) were obtained from the Rapp 360 \times 360 set of potential coefficients model determined from measured gravity anomaly data.⁸

The demonstration results are given in Table 5. The resulting position estimate error is 17.8 m in latitude and 21.7 m in longitude. These errors appear to be insensitive to the initial position offset of 100 m in each of the x , y , and z component directions. Computations were performed for several additional cases as a means to quantify the errors in the above estimates. These analyses assume the true location as an initial starting values as in case 2 of Table 4. The first correction is to use measured values for vertical deflections. These values ($\xi = -2.52$ arcsec and $\eta = 5.30$ arcsec) were obtained by the USNO⁹ using the Danjon astrolabe to an accuracy of about 0.1 arcsec. This improves the case 2 results to estimated position errors of 6.3 and 5.9 m

in latitude and longitude, respectively. Consequently, the largest error sources in the computation are the modeled vertical deflection errors. Next, case 2 is improved further by replacing the combined leveling and vertical deflection height difference values by the difference in height from GPS values (Note: this could not be done at the offset point, since Δh_{GPS} is very dependent on the assumed position). This reduces the estimated position error to 3.7 m and 3.6 m in latitude and longitude, respectively. This indicates that leveling is the second largest error source in the procedure and that GPS contributed relatively small errors.

TABLE 5. POSITION ERRORS OF PROCEDURE DEMONSTRATIONS USING THE TEST DATA

Case	Assumed Position Offset* (m)	Vertical Deflection	Latitude Error (m)	Longitude Error (m)
1	100	Modeled	17.798	21.660
2	0	Modeled	17.798	21.660

* See discussion in text.

SUMMARY

Several techniques that have the potential to determine absolute positions in the presence of SA have been considered. All use some form of differencing of the GPS phase data to remove the *dither* component from SA. Those that require an auxiliary measurement are less sensitive to the *epsilon* component also. The two primary limiting factors that prevent these techniques from being practical are the precision with which the time difference of arrival (TDOA) of the wavefront at the ends of the baseline can be measured. The current limit is about 0.005 cycle or 1 mm at L_1 . The other limiting factor is the distance between the antennas. Since the TDOA measurement is essentially independent of the baseline length, a larger antenna separation gives a correspondingly more precise angular measurement. Baselines on the kilometer scale or larger are required for accurate estimates of the absolute position.

REFERENCES

1. Braasch, Michael S., *A Signal Model for GPS*, NAVIGATION: Journal of The Institute of Navigation, Vol. 37, No. 4, Winter 1990-1991.
2. Rapp, Richard H., Geometrical Geodesy, Part II, The Department of Geodetic Science and Surveying, The Ohio State University, Columbus, Ohio, September 1989, p.152.
3. O'Leary, Erin M., Alan G. Evans, and T. Nathan Smith, *An Evaluation of the Use of GPS and Laser Ranging to Position Stationary Objects from a Distance*, Proceedings of the 48th Annual Meeting of the Institute of Navigation, Washington, DC, June 1992.
4. Nassau, Jason, J., Practical Astronomy, McGraw-Hill Book Company, Inc., 1948, p84.
5. Heiskanen, W. and H. Moritz, Physical Geodesy, W. H. Freeman and Company, San Francisco, CA, 1967.
6. Evans, A. G., T. Solar, L. D. Hothem, et al., *Vertical Deflections and Astronomic Azimuth Derived from GPS and Leveling: Joint Test Description and Results*, Fifth International Geodetic Symposium on Satellite Positioning, Las Cruces, NM, March 1989.
7. Solar, T., A. E. Carlson, Jr., and A. G. Evans, *Determination of the Deflection of the Vertical Using GPS and Geodetic Leveling*, Geophysical Research Letters, **16**, No.7, pp 695-698, July 1989.
8. Solar, T., L. D. Hothem, A. G. Evans, and B. R. Hermann, *GPS Methods Vs Conventional Geodetic Techniques. Preliminary Results from the Dahlgren Test*, (Presentation), Spring Meeting of the American Geophysical Union, Baltimore, MD, May 1988.
9. Lukac, C., R. Keating and R. Clarke, *Deflections of the Vertical at MBRE Site, Dahlgren, Virginia*, U.S. Naval Observatory, Washington, DC, 1990.

DISTRIBUTION

	Copies	INTERNAL	Copies
DOD ACTIVITIES (CONUS)			
ATTN B BROTH DGF	1	E231	3
DEFENSE MAPPING AGENCY		E232	2
SUITE 200		E281 (HALL)	1
12100 SUNSET HILLS RD		K	1
RESTON VA 22090-3221		K10	1
		K12	1
ATTN S MALYS D54	1	K12 (HERMANN)	5
DEFENSE MAPPING AGENCY		K13 (EVANS)	5
4600 SANGAMORE RD		K13	1
BETHESDA MD 20816-5003		N74 (GIDEP)	1
DEFENSE TECHNICAL	12		
INFORMATIONCENTER			
CAMERON STATION			
ALEXANDRIA VA 22304-6145			
CENTER FOR NAVAL ANALYSES	1		
HUDSON INSTITUTE INC			
PO BOX 16268			
ALEXANDRIA VA 22302-0268			
ATTN GIFT AND EXCHANGE			
DIVISION	4		
LIBRARY OF CONGRESS			
WASHINGTON DC 20540			

REPORT DOCUMENTATION PAGE

Form Approved
OMB No. 0704-0188

Public reporting burden for this collection of information is estimated to average 1 hour per response, including the time for reviewing instructions, searching existing data sources, gathering and maintaining the data needed, and completing and reviewing the collection of information. Send comments regarding this burden estimate or any other aspect of this collection of information, including suggestions for reducing this burden, to Washington Headquarters Services, Directorate for Information Operations and Reports, 1215 Jefferson Davis Highway, Suite 1204, Arlington, VA 22202-4302, and to the Office of Management and Budget, Paperwork Reduction Project (0704-0188), Washington, DC 20503.

1. AGENCY USE ONLY (Leave blank)	2. REPORT DATE September 1993	3. REPORT TYPE AND DATES COVERED Final	
4. TITLE AND SUBTITLE ABSOLUTE POSITIONING BY COLLECTING GLOBAL POSITIONING SYSTEM (GPS) DATA ALONG SHORT BASELINES		5. FUNDING NUMBERS	
6. AUTHOR(S) Bruce R. Hermann and Alan G. Evans		8. PERFORMING ORGANIZATION REPORT NUMBER NSWCDD/TR-93/309	
7. PERFORMING ORGANIZATION NAME(S) AND ADDRESS(ES) Naval Surface Warfare Center, Dahlgren Division (Codes K12/K13) Dahlgren, VA 22448-5000		10. SPONSORING/MONITORING AGENCY REPORT NUMBER	
9. SPONSORING/MONITORING AGENCY NAME(S) AND ADDRESS(ES)		11. SUPPLEMENTARY NOTES	
12a. DISTRIBUTION/AVAILABILITY Approved for public release; distribution is unlimited.		12b. DISTRIBUTION CODE	
13. ABSTRACT (Maximum 200 words) This report addresses the problem of determining absolute positions (longitude and latitude) from Global Positioning System (GPS) data in the presence of Selective Availability (SA). The SA-epsilon effect can be avoided if one can wait until corrected or post-fitted satellite ephemerides and clock estimates become available. However, the SA-dither effect cannot easily be eliminated from the ranging data in the field. This report considers both problems and suggests methods that have the potential to allow absolute position solutions to be obtained even with dither corrupting the satellite data. The requirements and practicality of each are reviewed.			
14. SUBJECT TERMS Selective Availability (SA) AntiSpoofing (AS) Absolute Positioning Global Positioning System (GPS)		15. NUMBER OF PAGES 33	
		16. PRICE CODE	
17. SECURITY CLASSIFICATION OF REPORT UNCLASSIFIED	18. SECURITY CLASSIFICATION OF THIS PAGE UNCLASSIFIED	19. SECURITY CLASSIFICATION OF ABSTRACT UNCLASSIFIED	20. LIMITATION OF ABSTRACT UL